International Journal Of Renewable Energy Research, IJRER
Z.Varga, P.Stumpf, R.K.Járdán, I.Nagy, Vol.1, No.4, pp.200-211 ,2011

Application of Ultrahigh Speed Induction Machine for Waste or Renewable Energy Recovery

ZoltánVarga, Péter Stumpf, Rafael K. Járdán, István Nagy‡

* Department of Automation and Applied Informatics, Budapest University of Technology and Economics, Hungary

‡ IstvánNagy,Tel: +36 1 463 1409, Fax: +36 1 463 1 3163, e-mail: varga.zoltan@mail.bme.hu, stumpf@get.bme.hu, jrk@elektro.get.bme.hu, nagy@get.bme.hu

Invited Paper

Abstract-Applications of Ultrahigh Speed Induction Machine (USIM) in a system developed for utilization of renewable and waste energies is described. It can be applied in Distributed Generation Systems. The energy conversion is made by a turbine-generator set. USIM has a number of technical and economical benefits over synchronous generators. The following studies are presented: scalar speed control of the turbine-generator set applying an accurate and approximate model, the adverse effect of subharmonics generated by the PWM controlled voltage source converter and a novel self-excitation method developed specially for ultrahigh speed induction generators.

Keywords-Waste Energy Recovery System, Ultrahigh Speed Drive, Subharmonics, Self Excitation.

1. Introduction

In recent years, due to the shrinking energy resources facing mankind, the increased demand for more energy and the protection of environment, have led to intensive search for environment-friendly ways of energy production. A novel trend in electric power production is the application of small scale, low power plants (Disperse Power Plants, DPPs), utilizing local energy sources by micro-turbine system (<50kW), saving the cost of power transmission and distribution [3,4,7,8,9,22, 30, 34].

The system presented in this paper has been developed basically for utilizing a range of waste energies and renewable energy resources. Fields of application of the system described include most of the alternative renewable energy sources that are suitable for producing saturated or superheated steam or gas with low or medium pressure. The alternative renewable energy sources include solar energy (direct solar steam system or binary cycle system), geothermal energy and energy obtained from biomass. Various waste energy sources can also be utilized by applying the system presented. The system can be operated in island or grid connected mode.

Due to the fast development of manufacturing technologies high speed generators can be manufactured and latest development of power electronic devices resulted in the appearance of ultra high speed induction machines (USIM) in electric power generation that offers reduced sizes, increased efficiency and the possibility to match the speed of the generator and the turbine.

The current paper is a review of the work done by the authors in the publications [1-4].

2. Description of the System

Assuming an application in a steam network, the basic set-up and operation will be described briefly by a simplified block diagram of the system, shown in Fig. 1 for the case of parallel operation with the utility network. The working medium (steam) fed to the turbine T through a control valve produces torque driving the USIM. The electric power generated by USIM at varying voltage level and frequency is to be fed to the utility mains via the DC link converter, consisting of two three-

phase converters (CONV-1 and CONV-2). The*Brake Chopper* absorbs the kinetic energy when the system is turned off normally or in fault conditions.

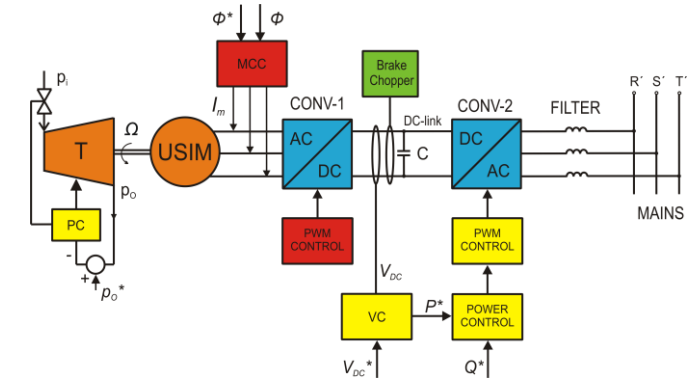

Fig 1. Functional block diagram of the system studied

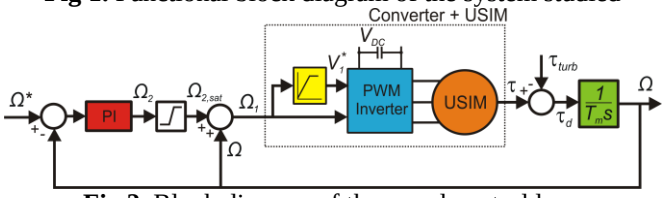

Fig 2. Block diagram of the speed control loop

The system incorporates a number of control loops, the most important ones are the pressure controller (PC) and the active power controller loops. A pressure controller loop keeps the outlet pressure p_o of the working medium constant, corresponding to a reference signal p_o^*. This function is necessary to ensure that the system can be used to replace throttle valves. The mechanical power generated is basically proportional to the $\Delta p=p_i - p_o$ pressure drop in the turbine, thus at varying inlet pressures the power that can be fed to the mains has to be controlled in order to keep power balance between the mechanical and electric sides.

The active output power of the converter is controlled according to a reference signal *P** of the control unit, given by the DC link voltage controller VC. The DC link converter topology applied, makes it possible to produce also reactive power *(Q)* for power factor correction and current waveforms for the elimination of higher harmonic currents. The amount of active and reactive power can independently be changed by varying the magnitude and the phase of the voltage space vector of converter *CONV-2* as compared to the space voltage vector of the mains. The output space voltage vector is defined by the PWM Control unit. The control unit Power Control, realized within the microprocessor controller, ensures that two variables (*P* and *Q*) will correspond to the reference signals *P** and *Q**, respectively.

The power balance between the power produced by the T-USIM set and the active power supplied to the grid can be ensured by the DC link voltage controller. Assuming an increase in V_{DC} as a result of increased turbine power, the DC link voltage control loop elevates the reference power *P**. This way it maintains constant DC link voltage that ensures the power balance between the mechanical and electrical sides.

There is another possibility for ensuring the power balance. Keeping the speed of the rotating machine set at a constant level the power balance is automatically ensured. One aspect of this solution will be treated in Section 4 and 5. In section 4 and 5 we assume that the speed control loop of USIM keeps the speed at constant level for power balance.

In the electric side the control of the unit *CONV-2* affects the output power fed to the utility mains. The power obtained from the working medium will be fed to the mains by changing the power reference signal *P** provided by the DC link voltage controller (VC).

3. Permanent Magnet Synchronous Generator (PMSG) versus Induction Machines

The electromechanical energy conversion in systems like the one studied in this paper is carried out most frequently by applying PMSGs. This is justified by a number of favourable properties of the PMSG. In the case of synchronous generator the magnetic field of the machine is ensured by the permanent magnets and the output voltage depends only on the speed and the load current. In the electrical energy conversion a simple diode rectifier can be connected to the output of the generator (in Fig.1 *CONV-1*), that is considerably cheaper, more robust and has higher efficiency as compared to the active PWM controlled AC/DC converter. As maintaining the magnetic field is associated with no losses, the efficiency of the synchronous machine (SM) is generally higher than that of the induction machine (IM). On the other hand the SM is more costly and ensuring synchronism in ultrahigh speed drives is more difficult task.

Applying IM offers a number of advantages. Up to medium power levels ultra high speed induction machines (USIMs) are produced in significant quantities e.g. for the machine tool industry as spindle drives, thus the price levels are generally attractive. The matured technology results in high reliability IMs.

The basic drawback of the IM is that in generating mode of operation maintaining of the magnetic field is more sophisticated when no voltage source is available to provide field current for the machine. In this case it can be ensured by applying an active PWM controlled AC/DC converter connected to the output of the IG (*CONV-1*), i.e. two identical back-to-back connected converters are needed for the electric energy conversion. The active AC/DC converter is considerably more expensive than the diode rectifier applicable with PMSG.

Instead of applying an active AC/DC converter, *CONV-1* can be a diode rectifier if the magnetic field is maintained by a separate Magnetizing Current Control Unit (MCC), which provides the magnetizing current for the USIM in such a way that a controller keeps either the stator flux or the stator voltage/frequency ratio constant by controlling the magnetizing current I_m.

In the following sections both solutions are studied briefly.

4. Speed Control of USIM

Due to the unusual parameters of USIM its working point might slip over to the unstable region during start-up or due to sudden increase of the driving turbine torque or sudden change in the speed reference signal. The second one is not relevant in the current application. Serious operation failure and system damage can be the result. Thus, a robust speed control loop to prevent overspeed is required. Though the optimum solution would be to use Field Oriented Control (FOC) for the induction machine, the converters applied in the laboratory does not make it possible to use FOC over a speed of 40 krpm. The rated speed of USIM in our case is 90 krpm, therefore we have to rely on *V/f* control to keep the stator flux constant.

The block diagram of the proposed speed control loop, known as Rotor Frequency Control (RFC), can be seen in Fig. 2. The output signal of the PI controller assumed to be the rotor angular frequency Ω_2. In practical applications the control loop actually includes a saturation block after the PI controller to limit the rotor angular frequency below the breaking value Ω_{2b} thus it can reliably be ensured that the machine cannot enter the unstable region. The synchronous speed Ω_1 can be obtained as the sum of Ω and Ω_{2sat}. The required stator voltage V_s to keeping the stator flux constant can be determined from Ω_1. At low frequencies a voltage boost is required due to the voltage drop across the R_s stator resistance to keep stator flux constant.

To obtain balanced three-phase output voltages with variable frequency and magnitude PWM converter control is used. The two most widely applied PWM techniques in the up-to-date converters are the sinusoidal carrier-based PWM technique (SPWM) applying a triangular carrier signal to compare against a reference sinusoidal waveform and the Space Vector Modulation (SVM) technique [6,10,11,18,19,35]. During the laboratory tests both methods were studied extensively, but in this paper SVM is assumed.

Based on the sampling pattern we distinguish Regular Sampling (RS) and Naturally Sampling (NS) methods. Regular Sampling is the most commonly used method in converters available in the market, because it is convenient to implement by Digital Signal Processor (DSP) or by microcontroller. In ultrahigh speed drives the high fundamental frequency f_1 and the limited carrier frequency (f_c *=12-20* kHz) results in low frequency ratio ($m_f = f_c/f_1 < 20$). For low m_f values Naturally Sampling is the better form of modulation than RS, as NS does not introduce distortion or a delayed response to the reference signal. NS techniques in the past was implemented by using analog devices, but nowadays with up-to date digital devices the accurate implementation of the NS-SVM techniques are also possible [1,6,10,11].

The dynamic torque $\tau_d = \tau - \tau_{turb}$ accelerates the USIM-turbine set where τ_{turb} is the turbine torque. The transfer function $\Omega/\tau_d = 1/(T_m s)$ gives the relation between the mechnical angular speed and dynamic torque τ_d, where $s=d/dt$ is the differential

operator and T_m is the electromechanical time constant.

A complete USIM and converter model with SVM in Matlab/Simulink environment was implemented. The USIM was modelled by using its direct- and quadrature axis (dq) representation [3,9].

To investigate the performance of the speed control loop an approximate model is also used. This simpler model is advantageous, because it takes considerably less computation time, while, as it will be shown later, it describes the transient operation of the speed control loop very similar to the accurate dq model. In the simpler model the electrical transients of USIM and converter are approximately taken into consideration by a one energy storage component with electric time constant T_e. The approximation is justified by the large electromechanical time constant T_m, that is, the slow mechanical transient process. Consequently the USIM can approximately be modelled by the refined nonlinear Kloss formula (KF), however, this formula basically is valid only in steady state condition.

The KF is given by [3]

$$\tau(\Omega_2) = \frac{2 \cdot \Omega_{2b} \cdot \Omega_2 \cdot (1+\varepsilon)}{\Omega_2^2 + \Omega_{2b}^2 + 2\varepsilon \cdot \Omega_2 \cdot \Omega_{2b}} \tau_{bm} \qquad (1)$$

whereτ_{bm} is the breaking torque in motoring operation and Ω_{2b} is rotor angular frequency belong to the maximal torque. Furthermore $\varepsilon = R_s / \sqrt{R_s^2 + X_r^2}$ and $X_r = X_r + X_{ls}X_m/(X_{ls}X_m)$, where *s* and *r* subscript denoting the stator and rotor values, *l* and *m* subscript denoting the leakage and mutual values. The Kfformula describes the operation of the USIM well at rated speed, where $R_s << X_r$, ε and Ω_{2b} is constant.

When the USIM does not operate at the rated speed (eg. during start-up) the frequency dependence of ε and Ω_{2b} has to be taken into consideration

$$\varepsilon = \frac{\Omega_1(T_0 - T')}{\sqrt{(1+(\Omega_1 T_0)^2)(1+(\Omega_1 T')^2)}} \qquad (2)$$

$$\Omega_{2b} = \frac{1}{T_{r0}} \sqrt{\frac{1+(\Omega_1 T_0)^2}{1+(\Omega_1 T')^2}} \qquad (3)$$

where

$$T_0 = \frac{L_{ls} + L_m}{R_s},\ T_{r0} = \frac{L_{lr} + L_m}{R_r},\ T_{r0} = \frac{L_{ls} + \dfrac{L_{lr}L_m}{L_{lr} + L_m}}{R_s}$$

T_0 is the time constant of stator currents, T_{r0} is the time constant of rotor currents when the rotor is open circuited and T' is the transient time constant of stator when the rotor is short circuited.

The T_e time constant of the one energy storage element is the transient time constant of the rotor when the stator is short circuited

$$T_e = T_r' = \frac{L_{lr} + \dfrac{L_{ls}L_m}{L_{ls} + L_m}}{R_r} \qquad (4)$$

Simulation Results

The simulations are performed in three steps: startup, stepwise changein the turbine torque $\tau_{turb}$and in the reference signalΩ^*.As it was mentioned previously a limiter is appliedafter the PI controller to keep the rotor frequency belowits breaking value Ω_{2b} by asafety margin. In this way themaximum torque of the USIM in motoring and generatingmode is also reduced. On the basis ofcontrol loop design and a series systematic simulationsthe recommended controller parameters are $K_p = 1$ and$T_i = 0.1$sec. In the paper simulation results will be shownonly for these parameter values.

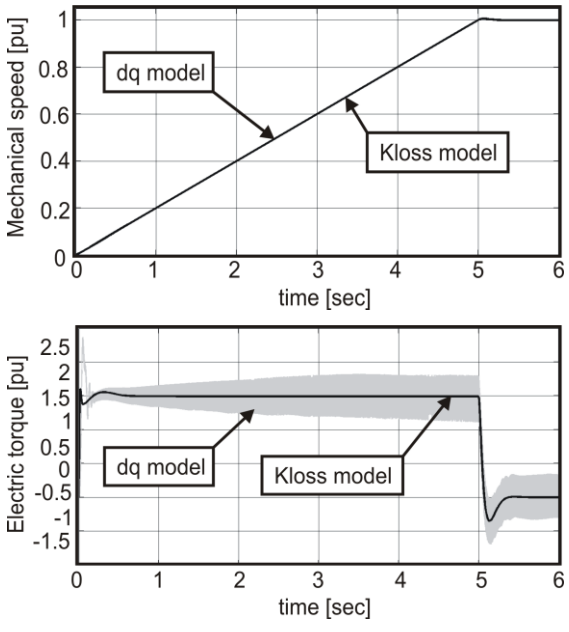

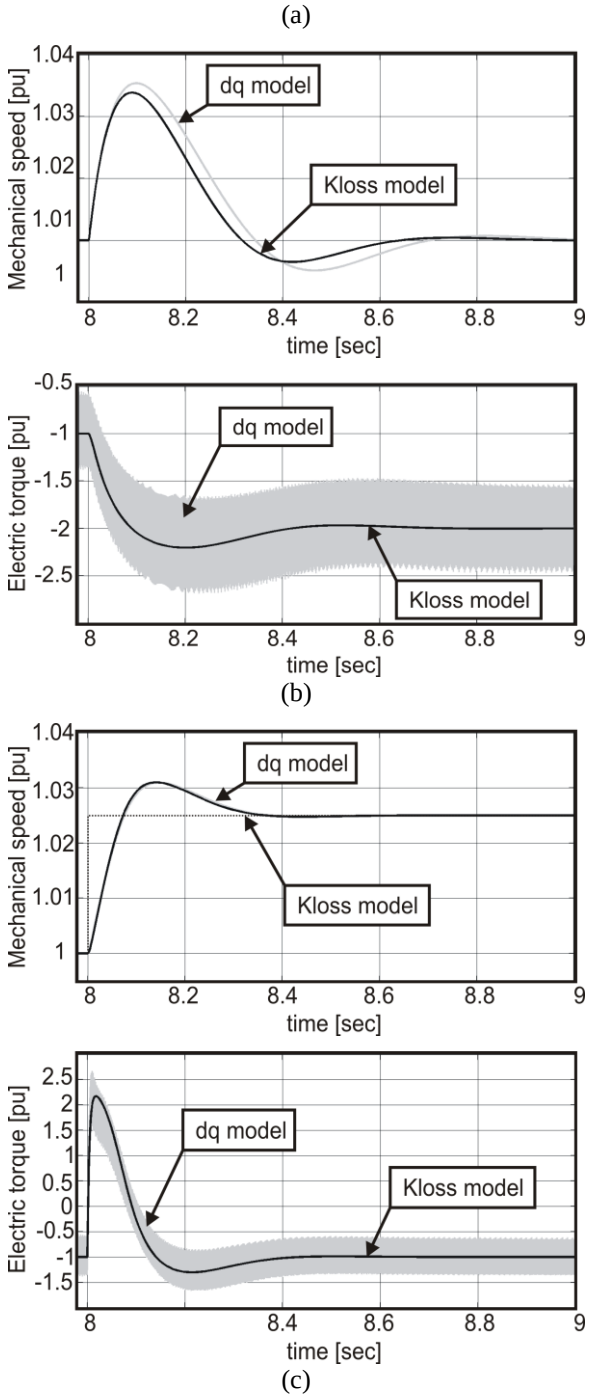

Fig.3. Transient response of the speed control loop, Simulation results.a)Startup, b)Sudden change in τ_{turb}($\Delta\tau_{turb}$=*-1* pu),c)Sudden change in Ω^* ($\Delta\Omega^*$ =*0.025* pu)

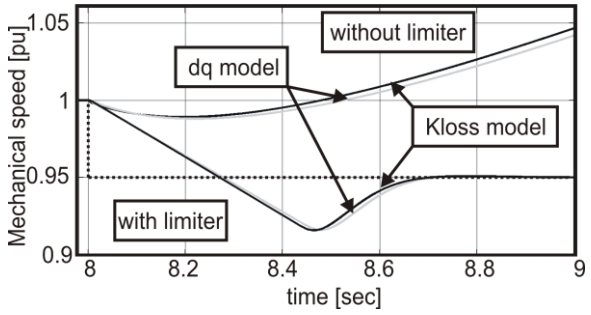

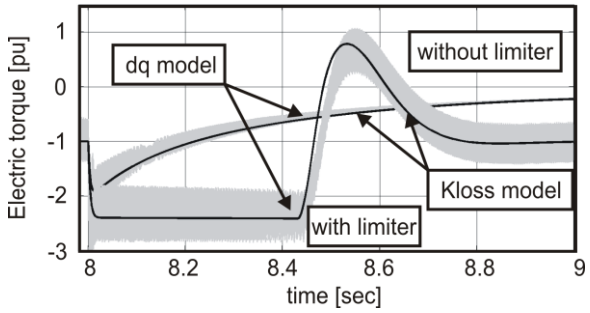

Fig 4. Response during sudden change in Ω* ($\Delta\Omega^*$ =*-0.05*pu) with and without limiter

The rated parameters of the USIM can be found in the Appendix.The total DC link voltagewas V_{DC} *= 650* V and the rated amplitude modulation index is$m_a = 2\sqrt{2}V_{LL,rms}/(\sqrt{3}V_{DC}) = 0.955$. The rated switching frequency of the converter available in the laboratory is f_c *=12* kHz, thus the rated frequency ratio is only m_f= 8. During the simulation RS-SVM is assumed.

Figure 3.shows the transient response of the speed control loop applying accurate dq-model with RS-SVM converter and simple Kloss model (KM), which does not take into consideration the generated harmonics by the PWM converter.

During start-up (Fig.3a) the USIM is operated as a motor supplied from the mains through the converters. The speed reference signal $\Omega^*$is varied as a ramp from zero up to its rated value. The inlet valve of the turbine is closed, so τ_{turb} = 0. The mechanical speed closely follows the reference signal $\Omega^*$and reaches the rated speed after a very small overshoot.

By applying accurate model the ripple of the electric torque τ during start-up is getting higher with Ω, but the average output torque is almost equals to the torque value determined by the Km. The reason is the following: at the beginning of the start-up process Ω_1 is small, thus the m_f frequency modulation ratio (f_c = *const.*) is high and the generated current harmonics by the PWM converter and the torque ripple are small. As the mechanical speed and the synchronous speed increases, the m_f decreases and the adverse effect of the harmonics becomes dominant.

As it can be seen at the beginning, when the frequency is small, the responses of the simpler KM and the accurate dqmodel in the electric torque somewhat differ, but as the frequency

increases the differences disappears and the curves coincide with each other.

Large sudden stepwise change in the turbine torque τ_{turb} or in the reference signal Ω^* provokes a dynamic process. The initial conditions of the transient process (Fig.3b and c) are $\Omega^* = 1$pu and $\tau_{turb} = -1$pu. Without a limiter after the PI controller a large sudden turbine torque increase or change in the reference signal might result in a serious operation failure. During acceleration Ω_2 can exceed Ω_{2b} and intrude into the unstable part of the speed-torque characteristics of USIM, where τ decreases with speed. The mechanical speed can reach dangerous levels. By applying the limiter the stability of the USIM can be ensured.

Figure 3b shows the response of the speed control when the sudden turbine torque change is $\Delta\tau_{turb}=-1$ pu. As it can be seen on the time functions of the mechanical speeds the resulting responses of the two USIM models are a tiny bit different, but the deviation is negligible and quantitatively the two responses are the same. Similarly to start-up the ripple of the electric torque τ is high, but the average output torque is almost equals to the torque value when KM is used.

Figure 3c shows the response of the speed control when the sudden reference signal change is $\Delta\Omega^*$=0.025 pu. The time functions of $\Omega(t)$ coincide with each other, the two models are working in the same way.

Figure 4 shows the response of the speed control loop with and without a limiter when a negative stepwise change ($\Delta\Omega^* = -0.05$pu) is applied in the reference signal. The limiter ensures the stability. The response of the dq model and the KM practically are the same. If the magnitude of the stepwise reference signal change is high, even if limiter is applied, oscillations with large amplitudes occur, which must be avoided. It is recommended to change the reference speed by a ramp signal both in positive and negative direction, or as in our case keep the speed reference constant.

It can be concluded that to investigate the performance of the speed control loop the approximate KM works well. It is advantageous, as it is simpler to follow the transient processes on the basis of steady-state characteristic and in addition it takes considerably less computation time.

5. Generation of subharmonics

The maximum carrier frequency of the converters available on the market is typically $f_{c,max} = 12 - 20$ kHz and generally their values can be changed in discrete steps. In a closed speed control loop, where the f_1 synchronous frequency is determined by the controller depending on the reference speed signal and the actual loading torque, the $m_f=f_1/f_c$ frequency ratio is not always integer. If the frequency ratio m_f is not integer subharmonics are generated. During the tests, considerable difficulties have been encountered in connection with the subharmonic fluxes generated with significant amplitudes and with very low frequencies by the PWM controlled converter (*CONV-1*) supplying the USIM. They can cause serious malfunction and breakdown in the USIM. To have a deeper insight, we started to research on the subharmonic generation when different PWM methods with different sampling techniques are applied [1,6].

The frequencies of the sideband harmonics grouped around the multiples of the carrier frequency f_c is

$$f_{harm} = (m \cdot m_f \pm n) f_1 \qquad (5)$$

where $m = 1,2,...$ and $n = 1, 2,\ldots$. One constraint is that when m is odd then $n = 2,4\ldots$ and when m is even then $n = 1,3\ldots$

The subharmonic component is the sideband harmonics of the first carrier harmonic group ($m = 1$) intruding below the fundamental. The subharmonic frequencies can be calculated from (5) ($m = 1$, $n = m_{f,int}$) as $f_{sub} = | f_c/f_1 - m_{f,int}| f_1$, where $m_{f,int}$ is the closest even integer frequency ratio belonging to f_1. For example at $f_1=1499.5$ Hz assuming the switching frequency is $f_c=12$kHz $f_{sub} = |12$ kHz$/1499.5$ Hz $-8| 1499.5 = 4$ Hz.

In [1] an efficient and especially convenient approach is used to study the subharmonic components of the converter output voltage space vector $\boldsymbol{v}_k$ obtained from the three output phase voltages of the converter. In this approach the time integral of $\boldsymbol{v}_k$ is calculated or measured, because its fundamental and harmonic components are

suppressed compared to the subharmonics due to their much higher frequencies. As its dimension is *Vsec*, it is called *"flux"* space vector and denoted by $\boldsymbol{\Psi}$. By Fourier expansion the subharmonic component $\boldsymbol{\Psi}_{sub}$ of $\boldsymbol{\Psi}$ is obtained and from $\boldsymbol{\Psi}_{sub}$ thesubharmonic voltage component $\boldsymbol{v}_{k,sub}$ of the space vector $\boldsymbol{v}_k$ can indirectly be determined. The methodsuppresses the disturbing "noise" generated by the voltage "jumps" in the output PWM voltage.

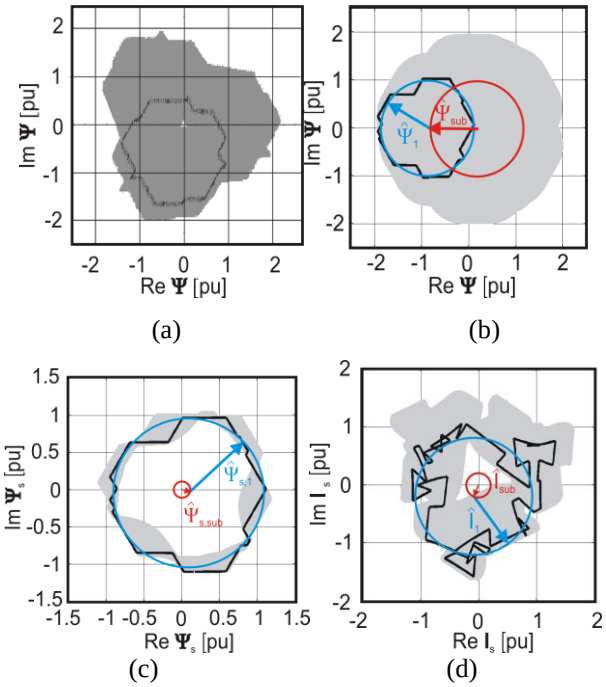

Fig.5. Trajectory of **Ψ**, **Ψs** and **Is**, RS-SVM, f_1=1499.5 Hz, $\hat{V}_{sub}$ = 0.8 V, f_{sub}=4 Hz. a)Trajectory of **Ψ**, Test result, b)Trajectory of **Ψ**, Simulation, c)Trajectory of **Ψs**, Simulation, d)Trajectory of **Is**, Simulation

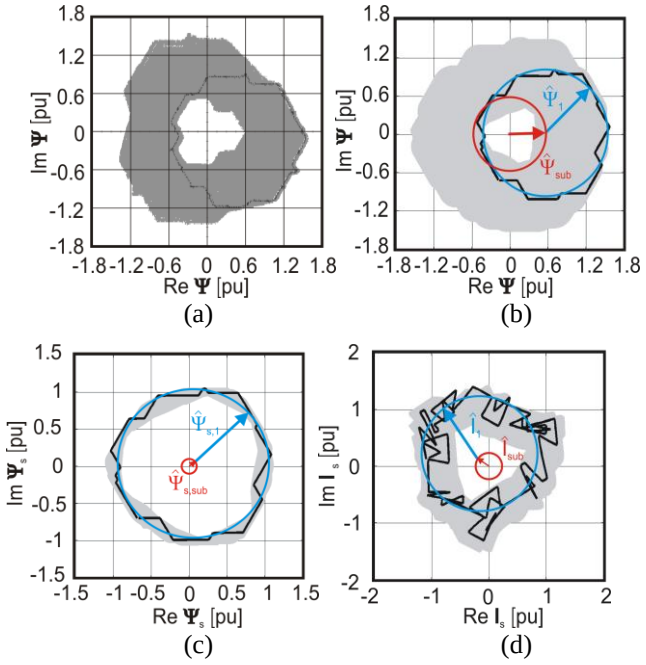

Fig.6. Trajectory of **Ψ**, **Ψs** and **Is**, RS-SVM, f_1=1499.5 Hz, $\hat{V}_{sub}$ = 0.8 V, f_{sub}=4 Hz. a)Trajectory of **Ψ**, Test result, b)Trajectory of **Ψ**, Simulation, c)Trajectory of **Ψs**, Simulation, d)Trajectory of **Is**, Simulation

Let us consider the amplitude of the fundamental $\hat{V}_1$ and subharmonic voltage component $\hat{V}_{sub}$. By neglecting the stator resistance, these voltage components result in flux components with amplitude $\hat{\Psi}_1 = \hat{V}_1/\omega_1$ and $\hat{\Psi}_{sub} = \hat{V}_{sub}/\omega_{sub}$, where $\omega_1 = 2\pi f_1$ is the fundamental and $\omega_{sub} = 2\pi f_{sub}$ is the subharmonic angular frequency.The ratio of the amplitudes is

$$\frac{\hat{\Psi}_{sub}}{\hat{\Psi}_1} = \frac{\hat{V}_{sub}}{\hat{V}_1}\frac{\omega_1}{\omega_{sub}} \qquad (6)$$

If ω_{sub} is small enough, $\hat{\Psi}_{sub} > \hat{\Psi}_1$ can be the result. In the case studied, the frequency of the significant subharmonic component is two to three orders of magnitude lower as compared to that of the fundamental component; thus, a subharmonic voltage component with amplitude of 10^{-3}pu magnitude results in a subharmonic flux that is comparable to the fundamental component.

The amplitude of the subharmonic components can be calculated from the equations derived in [6] for different PWM methods and sampling techniques.

Theoretically by applying RS-SVM the amplitude both the subharmonic voltage and resulted subharmonic flux components are negligible. Contrary to the theory our finding was that the RS-SVM does generate subharmonic flux with considerable amplitudes. The reason of the subharmonics can be the imperfect operation of the PWM controller. Furthermore the distortion of the output voltage waveform could be caused by side effects (like discrepancies in control algorithm, voltage drops and limited switching times of the switching devices, blanking times, etc.).

Figure 5a and 6a show a measured trajectory of $\boldsymbol{\Psi}$when m_f= *8.0027* (f_1 = *1499.5* Hz) andm_f= *10.0025* (f_1 = *1199.7* Hz), respectively. The amplitude and the frequency of the measured subharmonic voltage components are $\hat{V}_{sub}$= 0.8 V = $2.5\cdot10^{-3}$pu, f_{sub}=*0.0027* pu= *4* Hz (Fig.5a) and

$\hat{V}_{sub}$= 0.3 V = 9.6·10^{-4}pu, f_{sub}= *0.002* pu= *3* Hz (Fig.6a). By neglecting the stator resistances thesesubharmonic voltage components result in flux componentswith amplitude $\hat{\Psi}_{sub}$= 0.97 pu (Fig.5a) and $\hat{\Psi}_{sub}$= 0.48 pu (Fig.6a).

The subharmonic voltage components obtained by tests are added to the output voltage of the RS-SVM controlled converter in the simulation model to investigate their effects by simulation. Figure 5b and 6b shows the trajectory of $\boldsymbol{\Psi}$when the reference speed is Ω^*=*1.0058*pu and Ω^*=*0.8056*pu, respectively. Near rated load torque the f_1 synchronous frequency determined by the controller are f_1=*0.9997* pu=*1499.5* Hz (Fig.5b) and f_1=*0.7998* pu=*1199.7 Hz* (Fig.6b). As it can be seen the trace of $\boldsymbol{\Psi}$obtained by test and simulation are similar.

Figure 5c and 6c show the trajectory of the stator flux of USIM denoted by Ψ_s when theR_s stator resistance is taken into consideration. The amplitude of the subharmonicstatorflux vector $\hat{\Psi}_{s,sub}$is considerably smaller ($\hat{\Psi}_{s,sub}$=0.07 pu in Fig.5c and $\hat{\Psi}_{s,sub}$=0.03 pu in Fig.6c) than that of $\hat{\Psi}_{sub}$clearly indicating that the stator resistance is not negligible at f_{sub}.The explanation is the follows: the small subharmonic frequency f_{sub} of the subharmonic voltage components results in verysmall magnetizing and leakage reactances at f_{sub}. It causes that the per-phase equivalent impedance of theUSIM at the subharmonic frequency is very small and the value of stator resistance dominates in it. Thesubharmonicvoltage $\hat{V}_{sub}$ across the small per-phase equivalent impedance at f_{sub} generates subharmonic currents with considerable amplitudes as it can be seen in Fig.5d and Fig.6d, where $\hat{I}_{s,sub}$ = *0.3*pu and $\hat{I}_{s,sub}$= *0.12*pu.

The NS-SVM is prone to generate subharmonics with considerable amplitudes than RS-SVM. Furthermore NS-SVM generatesDC voltage components in the stator phase voltagesof USIM when m_f is even integer and it is not multiple of 3.The currents generated by the DC voltage components can bevery high due to the small stator resistance. The results verified by laboratory measurements are discussed in more detail in [1].

6. Novel Self-Excitation Method of USIM

As it was mentioned previously, by the self-excitation of the USIM we can avoid the need for the expensive active PWM AC/DC converter (CONV-1 in Fig.1) and the problems related to the subharmonics generation. In this case CONV-1 can be a low cost diode rectifier. A widely applied solution for self-excitation is to connect proper amount condensers to the stator terminals of the induction machine to ensure the magnetizing current. This solution is only applicable at a narrow range of load and speed levels, for a wider range a stable self-excitation can only be ensured by a more sophisticated control strategy, that is able to control the stator flux according to the requirements determined by the speed and load. A number of examples for the application of self-excited induction generators (SEIGs) are found in systems developed for utilization of wind energy and further applications are presented in [12-15].

The single phase equivalent circuit of the self-excited IG with condenser at its input is shown in Fig. 7. The value of the inductive reactance varies proportionally, while that of the capacitive reactance varies inversely with the ω_1 synchronous angular frequency. The magnetizing current necessary for keeping constant stator flux is fairly independent of frequency, while the capacitive current provided by the capacitor is changing inversely proportional to the square of the stator frequency of the machine. That explains the very limited range of operation with constant condenser value. Solutions have been suggested to use two or more condensers periodically connecting them in parallel [15]. The solution is viable, but it has drawbacks, it is hard to get a stable control system and the output voltage waveform of the generator is distorted and contains step-wise changes.

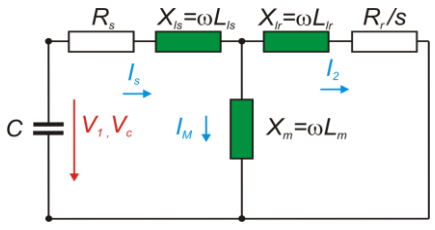

Fig.7. Single phase equivalent circuit of the self-excited induction machine

The principle of operation of the novel self-excitation method is based on controlling the magnetizing current continuously by applying a series or a parallel *L-C* branch. Here the value of the L_2 inductance is varied by high frequency PWM control (see Fig.8). Selecting the value of the condenser for the lowest frequency and the highest magnetizing current, the resulting capacitive reactance needs only reduction in other working points. A variable "virtual" capacitive reactance is realized in such a way, that not the capacitance is varied but rather the inductive reactance of a series connected inductor. Neglecting the losses of the reactive components, the resulting reactance is the difference of the capacitive and the inductive reactance. Assuming series *L-C* branch and varying *L*, when measuring the resulting reactive reactance, we realize a variable capacitive reactance. At constant frequency and zero value of the controlled inductanceL_2 at $D = 1$, (where $D = t_{on}/T_s$, is the duty ratio) maximum capacitive reactance is measured, furthermore at the maximum value of the inductance L_2 ($D = 0$), the resulting reactance is minimum, providing maximum magnetizing current. By applying parallel *L-C* branch at $D=0$ the resulting reactance of the parallel connected *C* and L_1 is minimum providing maximum magnetizing current. At the maximum value of inductance L_2 ($D=0$) the resulting reactance of *C* and L_1+L_2 is maximum, providing minimum magnetizing current.

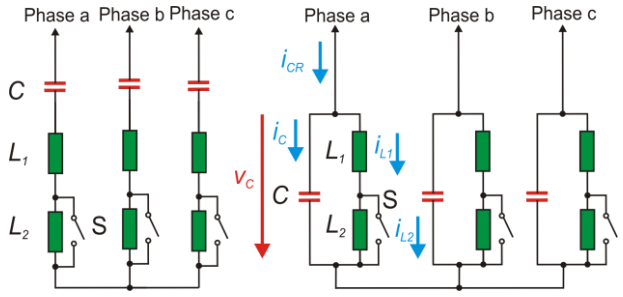

Fig.8. PWM controlled series and parallel L-C excitation of the FCC

The frequency range of operation of the MCC system is chosen in such a way that the stator frequency is below the resonant frequency of the *L-C* circuit, thus the resulting reactance remains capacitive.

At a given stator frequency range and a range of field current requirement, the value of the condenser and the inductances can be determined. The inductances L_1 are needed to limit the current ripple of the field currents and the peak currents of the switches. Depending on the level of the ripple current allowed, these inductances are approximately one order of magnitude smaller than the inductances L_2.

A closed loop feedback control ensures constant stator flux or controls the terminal voltage of the IG proportional to the stator frequency controlling the field current of the machine as required at a given frequency and load. In the practical implementation the principal circuit arrangement is realized in such a way that the common points of the inductances L_1 and L_2 are connected to the ac input terminals of a separate three diode bridge, while the dc output is connected to the Drain-Source terminals of an IGBT controlled by a PWM controller, thus the inductors L_2 are periodically short circuited. A D-R-C snubber circuit is used at the dc output of the diode bridge to limit over voltages. The operation of this arrangement is identical to the one in Fig.8, but the cost of material is reduced by saving two IGBTs and their control circuits (the cost of the additional diode bridge is lower).

The design process of the MCC for series and parallel *L-C* branch for USIM is described in [3,4]. Here we only refer to them. Assuming parallel *L-C* branch and the parameters of the USIM (see Appendix) the calculated numerical values of the elements in the MCC unit are: $L_1 = 0.1$mH, $L_2 = 8$mH, the capacitor: C = 2.23μF [4].

In Fig. 9 simulation results obtained by using PSpiceare presented assuming the parameters listed previously and the parallel *L-C* circuit arrangement (Fig.8b). The stator frequency is $f_1=1500$ Hz, the duty ratio $D = 0.25$. In order to limit current ripple, a switching frequency of $f_s = 30$ kHz has been applied. Figure 9 shows theresulting current i_{CR} of the parallel *L-C* branch(Fig.8b), the current of the condenser i_c, the two inductor currents i_{L1} and i_{L2}, and the voltage of the condenser v_c. As it can be seen the resultant current i_{CR} and the current of the condenser lead the condenser voltage v_c with 90°. The amplitudeof the resultant current i_{CR} can be varied with the duty ratio *D*.

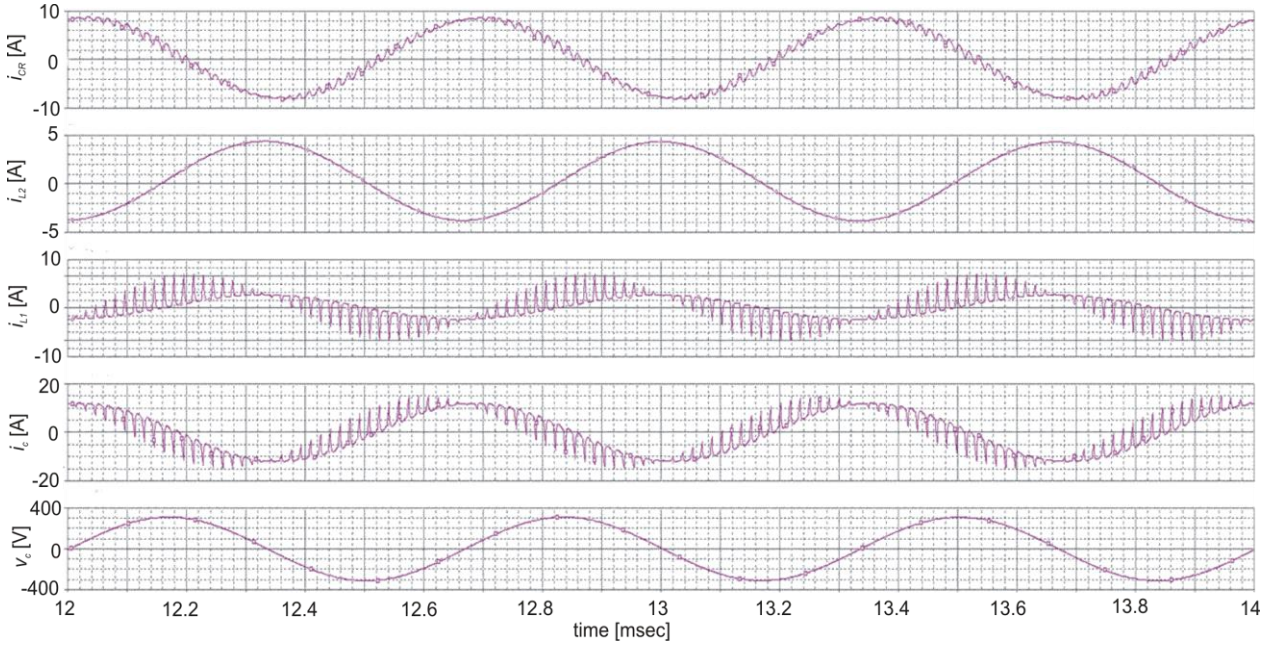

Fig.9. Simulation results. $f_1 = 1500$ Hz, D = 0.25, $f_s = 30$ kHz, time function of i_{CR}, i_{L2}, i_{L1}, i_C and v_C

7. Conclusion

Research results obtained during the development of a system that can be applied to utilize renewable and waste energies in Distributed Power Systems have been presented. The work described is aimed at developing solutions that make it possible to apply Ultrahigh Speed Induction Machines (USIM) for the electromechanical conversion in the energy system.

The simulation results of the speed control loop have been summarized. The significance of the study stems from extreme sensitivity of the USIM for overspeed. The paper presents an approximate model to describe the operation of the USIM. As the simulation results show, assuming an ideal converter the results of the approximate model and the widely-used accurate dq model are very similar. Thus, to investigate the performance of the speed control loop the approximate model is suitable. It is advantageous, as it is simpler to follow the transient processes on the basis of steady-state characteristics and in addition the application of the approximate model takes considerably less computation time.

In the paper it was shown that the subharmonics due to the imperfect operation of the PWM controller can result subharmonic flux and current components with considerable amplitudes. They can cause serious malfunction of the machine.

Furthermore a novel self-excitation method developed makes it possible to control the stator flux of the IG by controlling the magnetizing current continuously, ensuring a stable self-excitation in a wide range of speed and load. By the novel self-excitation method the investment cost of the system can be reduced and the problems connected to the subharmonics can be avoided.

Acknowledgements

The authors wish to thank the Hungarian Research Fund (OTKA K72338) and the Control Research Group of the Hungarian Academy of Sciences (HAS).

This work is connected to the scientific program of the ”Development of quality-oriented and harmonized R+D+I strategy and functional model at BME” project, furthermorethe project is supported by the New Széchenyi Plan (Project ID: TÁMOP-4.2.1/B-09/1/KMR-2010-0002)

References

[1] P. Stumpf, R. K. Jardan, I. Nagy, “Subharmonics generated by Space Vector Modulation in Ultrahigh Speed Drives”, IEEE Transactions on Industrial Electronics, Vol. 59, No. 2., pp. 1029-1037, February, 2012

[2] P. Stumpf, R. K. Jardan, I. Nagy, „Dynamics of Different Speed Controls of Ultra High Speed Induction Generators Using Approximate and Accurate Model“, In Proceedings of SPEEDAM 2010, Pisa, Italy, pp. 1024-1029

[3] Z. Varga, R. K. Jardan, I. Nagy, “Investigation of Self-Excited Ultrahigh Speed Induction Generators for Distributed Generation Systems”, In Proceedings of ACEMP 2011, Istanbul, Turkey, pp. 565-570

[4] Z. Varga, R. K. Jardan, I. Nagy, “Ultrahigh Speed Induction Generators Applied in Disperse Power Plants”, In Proceedings of INTELEC 2011, Amsterdam, Netherlands, pp. 1-7, ISSN: 2158-5210

[5] M. G. Simoes, F. A. Farret, Renewable Energy Systems – design and analysis with induction generators, ISBN: 9-781-4200-5532-0, December 2007

[6] T. Lipo, G. Holmes, Pulse Width Modulation for Power Converters (Principles and Practice), Hoboken, NJ: Wiley, 2003.

[7] G. Iwanski and W. Koczara, “Power management in an autonomous adjustable speed large power diesel gensets,” in Proceedings of EPE-PEMC, Poznan, Poland, Sep. 1–3, 2008, pp. 2164–2169. 458

[8] J. Leuchter, P. Bauer, V. Hajek, and V. Rerucha, “Dynamic behaviormodeling and verification of advanced electrical-generator set concept,” IEEE Trans. Ind. Electron., vol. 56, no. 1, pp. 266–279, Jan. 2009.

[9] M.Mirošević, Z. Maljković, D.Pavlinović, “The Dynamics of Diesel-Generator Unit in Isolated Electrical Network”, International Journal of Renewable Energy Research, IJRER Vol.1, No3, pp.126-133, 2011

[10]A. Julian and G. Oriti, “Three-phase VSI with FPGA-based Multisampled Space Vector Modulation,” IEEE Transactions on Industry Applications, vol. 47, no. 8, pp. 1813–1820, August 2011.

[11]D. Rus, N. Preda, I. Incze, M. Imecs, and C. Szabo and, “Comparative Analysis of PWM techniques: Simulation and DSP Implementation,” in Proceedings of IEEE International Conference on Automation Quality and Testing Robotics (AQTR) 2010, pp. 1 –6., May 2010

[12]Karthikeyan A., Nagamani C., Ilango C.S., SreenivasuluA.,”Hybrid, open-loop excitation system for a wind turbine-driven stand-alone induction generator”, Renewable Energy Power Generation, IET, 10 March 2011, pp. 184-193

[13]Chauhan Y.K., Jain S.K., Singh B.,”A Prospective on Voltage Regulation of Self-Excited Induction Generators for Industry Applications”, IEEE Transactions on Industrial Applications, Vol. 46, 15 January 2010, pp. 720-730

[14]Kishore A., Prasad R.C., Karan B.M: “Design of Field Oriented Controller to Improve Dynamic Characteristics of Three Phase Self Excited Induction Generator”, In Proceedings of Conference on Industrial Electronics and Applications, 24-26 May 2006, pp. 1-6

[15]L. Robinson, D.G. Holmes, ”A Single Phase Self-Excited Induction Generator with Voltage and Frequency for use in a Remote Are Power Supply”, In Proceedings of AUPEC 2006, Melbourne, Australia, pp. 1-6

[16]S. Halasz and V. Zakharov, “Novel voltage spectra investigation of space vector modulation technique,” in Proceedings of the Annual Conference of Industrial Electronics Society IECON, November, 2003, pp. 2660-2666

[17]S. Halasz, “Voltage spectrum of pulse-width-modulated inverters,” PeriodicaPolytechnica Electrical Engineering, vol. 25, no. 2, pp. 135–145, 1981.

[18]M. J. Duran, T. Glasberger, D. Dujic, E. Levi, and Z. Peroutka, “A modified sector based space vector PWM technique for five-phase drives,” IEEJ Transactions on Electrical Engineering, vol. 4, no. 4, pp. 453–464, Jul. 2009, iSSN 1931-4973. John Wiley&Sons, Inc.

[19]V. Oleschuk, F. Profumo, and A. Tenconi, “Simplifying approach for analysis of space-vector PWM for three-phase and multiphase converters,” in Proceedings of 12th European Conference on Power Electronics and Applications, EPE2007, Aalborg, Denmark, Sep.2–5, 2007, pp. 1–10, CD Rom ISBN: 9789075815108

[20]B. Robert, H. H. C. Iu, and M. Feki, “Widening the stability range of a PWM inverter using a robust chaos control,” in Proceedings of the 10th European Conference on Power Electronics and Applications (EPE2003), Toulouse, France, Sep. 2–4, 2003, cD Rom ISBN:90-75815-07-7.

[21]R. Ramchand, K.Sivakumar, A. Das, C. Patel, and K. Gopakumar, “Improved switching frequency variation control of hysteresis controlled voltage source inverter-fed IM drives using current error space vector,” IET Power Electronics, vol. 3, no. 2, pp. 219–231, Mar. 2010.

[22]E. Vidal-Idiarte, L. Martinez-Salamero, H. Valderrama-Blavi, F. Guinjoan, and J. Maixe, “Analysis and design of Hinf control of nonminimum phase-switching converters,” IEEE Transactions on Circuits and Systems I: Fundamental Theory and Applications, vol. 50, no. 10, pp. 1316–1323, Oct. 2003.

[23]J. H. Chen, K. T. Chau, and Q. Jiang, "Analysis of chaotic behavior in switched reluctance motors using voltage PWM regulation," Electric Power Components and Systems, vol. 29, no. 3, pp. 211–227, Mar. 2001.

[24]Y. Zhou, P. Bauer, J. A. Ferreira, and J. Pierik, "Operation of grid connected DFIG under unbalanced grid voltage condition," IEEE Transactions on Energy Conversion, vol. 24, no. 1, pp. 240–246, Mar. 2009.

[25]S. Ryvkin, "Cutting out the voltage oscillation influence on the control quality of a three-level inverter drive by using sliding mode," in Proceedings of the 14th International Power Electronics and Motion Control Conference, EPE-PEMC2010, Ohrid, Republic of Macedonia, Sep. 6–8, 2010, pp. T3–6–T3–12, cD Rom ISBN: 978-1-4244-7854-5

[26]Z. Ye, P. K. Jain, and P. C. Sen, "Phasor-domain modeling of resonant inverters for high-frequency AC power distribution systems," IEEE Transactions on Power Electronics, vol. 24, no. 4, pp. 911–923, Apr. 2009.

[27]J. Dudrik and V. Ruš˘cin, "Voltage fed zero-voltage zero-current switching PWM DC–DC converter," in Proceedings of the 13th International Power Electronics and Motion Control Conference, EPE-PEMC2008, Poznan, Poland, Sep. 1–3, 2008, pp. 295–300, cD Rom ISBN: 978-1-4244-1742-1.

[28]V. Moreno-Font, A El Aroudi, J. Calvente, R. Giral, L. Benadero, "Dynamics and Stability Issues of a Single-Inductor Dual-Switching DC-DC Converter" IEEE Transactions on Circuits and Systems-I: Regular Papers, Vol 57, No. 2, February 2010, pp.415426

[29]Kolokolov Y, Ustinov P, Essounbouli N, Hamaoui A, "Bifurcation-free design method of pulse energy converter controllers", Chaos Solitons and Fractals, Vo1.42, No.5, 2009, pp. 2635-2644

[30]J.F. Baalbergen, P. Bauer, JA Ferreira, "Energy Storage and Power Management for Typical 4Q-load", IEEE Transactions on Industrial Electronics, Vo1.56, No.5, 2009, pp.1485-1498

[31]P.M. Lacko M. Olejar, 1 Dudrik, "DC-DC Push - Pull Converter with Tum-Off Snubber for Renewable Energy Sources", EDPE 2009, Dubrovnik, Croatia, 12-14 Oct, 2009, CD Rom ISBN: 953-6037-56-8

[32]D. Giaouris, S. BaneIjee, B. Zahawi, V. Pickert, "Stability Analysis of the Continuous-Conduction-Mode Buck Converter Via Filippov's Method" Circuits and Systems I. Regular Papers, IEEE Transactions on (Circuits an Systems I: Fundamental Theory and Applications, IEEE Transactions on, 2008, Vol 55, Issue 4, pp. 1084-1096

[33]Komrska, T., Zak, J., Ovaska, S., Peroutka, Z.: Computationally efficient current reference generator for 50-Hz and 16.7-Hz shunt active power filters. International Journal of Electronics. Vol. 97, No. 1, 2010, pp. 63 - 81. ISSN: 0020-7217. Taylor & Francis

[34]WlodzimierzKoczara, Nazar -AIKhayat, "Variable Speed Integrated Generator VSIG as a Modem Controlled and Decoupled Generation System of Electrical Power", EPE 2005, Dresden, Germany, 11-14 September, 2005, CD Rom ISBN: 90-7581-08-05

[35]P. N. Tekwani, R. S. Kanchan, K. Gopakumar, " Current-Error SpaceVector- Based Hysteresis PWM Controller for Three-Level Voltage Source Inverter Fed Drives" IEE Proceedings on Electric Power Applications, September 2005., Vo1.152, No.5, pp. 1283-1295

Appendix

Rated parameter of USIM

Symbol	Name	SI	pu
P_n	Power	4.5 kW	
$\hat{V}_1$	Peak value of phase voltage	310 V	1 pu
$\hat{I}_1$	Peak value of phase current	13.5	1 pu
f_{1n}	Rated frequency	1500 Hz	1 pu
$\hat{\Psi}_1$	Peak value of stator flux	32.8 mVsec	1 pu
τ_n	Rated torque	0.4805 Nm	1 pu
τ_{bm}	Maximum torque in mot. mode	1.156 Nm	
s_b	slip at max torque	0.0275	
s_n	rated slip	0.00642	
R_s	stator resistance	0.21 Ω	
R_r	rotor resistance	0.1565 Ω	
X_{ls}	stator leakage reactance	2.98 Ω	
X_{lr}	rotor leakage reactance	2.98 Ω	
X_m	magnetizing reactance	44.6 Ω	
p	number of pole pairs	1	
T_m	electromechanical time constant	7.46 s	